Vision Research 51 (2011) 2063–2070

Contents lists available at ScienceDirect

Vision Research

journal homepage: www.elsevier.com/locate/visres

Visual function and white matter microstructure in very-low-birth-weight (VLBW) adolescents – A DTI study

Susanne Lindqvist [a,c], Jon Skranes [a,d,*], Live Eikenes [b], Olav Haraldseth [b,e], Torstein Vik [a], Ann-Mari Brubakk [a,d], Torgil Riise Vangberg [f]

[a] Department of Laboratory Medicine, Children's and Women's Health, Norwegian University of Science and Technology, N-7489 Trondheim, Norway
[b] Department of Circulation and Medical Imaging, Norwegian University of Science and Technology, N-7489 Trondheim, Norway
[c] Department of Ophtalmology, St. Olav's University Hospital, 7006 Trondheim, Norway
[d] Department of Pediatrics, St. Olav's University Hospital, 7006 Trondheim, Norway
[e] Department of Diagnostic Imaging, MR-Center, St. Olav's University Hospital, 7006 Trondheim, Norway
[f] Department of Radiology, University Hospital of North Norway, Tromsø, Norway

ARTICLE INFO

Article history:
Received 1 March 2011
Received in revised form 22 June 2011
Available online 9 August 2011

Keywords:
Brain
Diffusion tensor imaging
Fractional anisotropy
White matter integrity
Very low birth weight
Preterm birth
Visual acuity
Corpus callosum

ABSTRACT

Premature birth is associated with visual impairments, due to both cerebral and ocular pathology. This study examined the relationship between cerebral white matter microstructure, evaluated by diffusion tensor imaging (DTI), and visual function, in 30 preterm born adolescents with very low birth weight (VLBW = birth weight ⩽ 1500 g) and an age-matched group of 45 term born controls. Visual acuity correlated positively with fractional anisotropy (FA) in corpus callosum and in frontal white matter areas in the VLBW participants, but not in the control participants. Callosal visual connections may play a more important role in the development of good visual acuity than previously acknowledged in preterm born children.

1. Introduction

Preterm birth and very low birth weight (VLBW: birth weight < 1500 g) reduces the child's prospects of normal visual development, greatly increasing the risk of blindness and severely reduced vision (Crofts, King, & Johnson, 1998). There is also a high prevalence of less dramatically reduced, but nevertheless subnormal visual acuity (below 1.0 in Snellen decimals) in preterm populations (Fledelius, 1981; Lindqvist et al., 2007).

Magnetic resonance imaging (MRI) has over the last two decades improved our knowledge of how severe visual disability in preterm born children can be caused by cerebral lesions such as periventricular leucomalacia (PVL) (Eken et al., 1995; Jacobson et al., 1998). Although the relationship between major neurological disabilities and PVL is strong (Olsen et al., 1997), correlations between brain lesions and minor neurodevelopmental dysfunctions have been more difficult to detect (Counsell et al., 2003; Krägeloh-Mann et al., 1999; Olsen et al., 1997). It has been suggested that the slight reduction in visual acuity commonly seen in preterm born children may have a cerebral origin even with normal conventional MRI findings (Cooke et al., 2004; Hellgren et al., 2007; Holmström, el Azazi, & Kugelberg, 1999; Pike et al., 1994). The use of advanced imaging techniques such as diffusion tensor imaging (DTI) has been proposed to help unravel possible correlations between neurological dysfunction and cerebral pathology in these high risk children (Hellgren et al., 2007; Hüppi & Dubois, 2006; Nagy et al., 2003; Toosy et al., 2004). DTI is a very sensitive method for investigating the integrity of white matter microstructure (Hüppi & Dubois, 2006) by measuring the direction and the magnitude of water diffusion (Brownian motions) in brain tissue (Basser, Mattiello, & LeBihan, 1994). DTI findings are commonly reported as changes in the fractional anisotropy (FA), a measure of the degree of directionality of water diffusion. In white matter, diffusion is largest parallel to the main direction of axons, and smaller perpendicular to them, where cell membranes and myelin sheaths restrict the diffusion of water molecules. Higher FA values signify a high degree of anisotropy or directionality (i.e. a large portion of the available water molecules diffuses along the same axis) and may indicate better axonal organisation and normal myelination (Hüppi & Dubois, 2006).

* Corresponding author at: St. Olav's University Hospital, Kvinne-barn-senteret 6.et., Olav Kyrres gate 11, N-7006 Trondheim, Norway.
E-mail address: jon.skranes@ntnu.no (J. Skranes).

0042-6989/$ - see front matter © 2011 Elsevier Ltd. All rights reserved.
doi:10.1016/j.visres.2011.08.002

FA values of white matter have been shown to be lower in VLBW than in control subjects (Vangberg et al., 2006), and lower values have been correlated to perceptual, cognitive, motor and mental health impairments (Skranes et al., 2007). It has also been possible to correlate reading ability and working memory to DTI findings in specific anatomical areas of the brain in non-VLBW populations (Klingberg et al., 2000; Nagy, Westerberg, & Klingberg, 2004). However, no study has previously investigated the potential relationship between visual acuity and white matter integrity evaluated with FA values in preterm born populations.

In normal adolescent and young adult populations, visual acuity will be 1.0 (in Snellen decimals) or better in approximately 95% of the subjects. Thus, 1.0 represents the lower limit of normality, rather than the expected value (Elliott, Yang, & Whitaker, 1995; Fledelius, 1981; Frisén & Frisén, 1981). In an earlier study we have reported monocular distance visual acuity (with best correction) below 1.0 in approximately a third of adolescents with VLBW, compared to 4% of control subjects (Lindqvist et al., 2007).

The aim of this study was to examine a possible relationship between brain DTI findings and visual function, in a group of VLBW and control adolescents, using a voxel-based morphometric (VBM) regression analysis, to test the hypothesis that there is a relationship between white matter microstructure and vision in VLBW adolescents. Comparing visual abilities and white matter microstructure in children born preterm may help us to better understand the origin of impairments in prematurity, as well as increase our knowledge of normal visual development.

2. Material and methods

2.1. Subjects

This is a population based follow-up study of a group of preterm born 14-year old adolescents with very low birth weight (VLBW = birth weight $\leqslant$1500 g), and an age-matched control group of adolescents born at term with normal birth weight.

2.2. VLBW group

In 1986–1988, 121 VLBW children from the two Norwegian counties of Nord- and Sør-Trøndelag were admitted to the neonatal intensive care unit at the University Hospital in Trondheim. Of the 121 admitted children, 33 died, one child with trisomy 21 was excluded and six had moved out of the region at the time of assessments. Of the remaining 81, 46 (57%) attended both the cerebral MRI and the ophthalmological examination. DTI failed in 16 cases due to signal dropouts and distortions – most caused by the use of dental braces, motion or incorrect slice position. In 30 VLBW subjects (14 males and 16 females) both DTI and ophthalmological data were available. There were no differences in birth weight, gestational age, birth head circumference, anthropometrics at follow-up, MRI assessment age, mother's education and social class between the participating VLBW adolescents with and without DTI available. Four of the VLBW subjects had mild to moderate cerebral palsy (three walking and one not walking spastic diplegia). As the aim of our study was to find a correlation between visual function and varying degrees of structural integrity of white matter we did not exclude participants with known brain lesions.

2.3. Control group

The control group was born in the Trondheim region from the same birth cohorts as the VLBW children. Their mothers were enrolled before week 20 of pregnancy in a large multicenter study from which a 10% random sample of participating women (para 1 and 2) was selected for follow-up during pregnancy. At birth, all the children born to mothers in the random sample were included for follow-up. The control group comprised 122 term born children with a birth weight $\geqslant$ 10th percentile for gestational age, born to mothers in the 10% random sample. At follow-up, 10 had moved and two were excluded due to congenital malformations (one Goldenhaar syndrome and one congenital anomaly of the urinary system). Of the remaining 110, 55 (50%) consented to both MRI scanning and ophthalmological examination. Ten MRI scans had to be excluded (because of dental braces, movement artefacts or missing imaging sequences), leaving 45 MRI investigations suitable for DTI analysis (17 males and 28 females). Some characteristics of the children in the two study groups are summarised in Table 1. The study was carried out in keeping with the guidelines of the Declaration of Helsinki. The Regional Committee for Medical Research Ethics approved the study protocol. Written informed consent was obtained from both adolescents and parents.

2.4. Visual assessment

We have previously reported that visual acuity, contrast sensitivity and several binocular functions were poorer in the VLBW than in the control group (Lindqvist et al., 2007, 2008). No media opacities were found, none had retinal pathology suggestive of earlier severe retinopathy of prematurity and none had been treated in infancy with cryo- or laser-therapy for severe retinopathy of prematurity (Lindqvist et al., 2007). The ophthalmologist performing the examination was blinded to group assignment.

The image acquisition was performed approximately half a year after the ophthalmological exam (see Table 1), with controls and VLBW adolescents in a random mix. Technicians and radiologists were blinded to group allocation during image acquisition.

2.5. Selection and processing of visual variables

The visual variables with statistically significant differences in performance between the VLBW and the control group ($p < 0.05$) which were selected for analysis of correlations to FA values were: best corrected distance visual acuity, near point of convergence, stereopsis (all as continuous variables), contrast sensitivity (as a discrete variable) and strabismus (as a dichotome variable). The mean value of the best corrected distance visual acuity of the right and left eye was used, since information in all visual fibres post chiasm will be a mixture of equal proportions originating in the right and left eye.

2.6. Image acquisition

All subjects were scanned in a 1.5 T Siemens Magnetom Symphony with Quantum gradients (30 mT/m) and a quadrature head coil. The protocol consisted of a structural T_1-weighted magnetisation-prepared rapid-acquisition gradient-echo (MPRAGE) sequence with TR = 7.1 ms, TE = 3.45 ms, TI = 1000 ms, flip angle 7°, FOV 256 $\times$ 256 mm and slab thickness 170 mm. The acquisition matrix was 256 $\times$ 192 $\times$ 128, reconstructed to 256 $\times$ 256 $\times$ 128, giving a reconstructed voxel resolution of 1 $\times$ 1 $\times$ 1.33 mm. The DTI sequence was a single-shot balanced-echo EPI sequence that significantly reduces eddy current distortions compared to a Stejskal–Tanner sequence (Reese et al., 2003). Timing parameters were TR = 6000 ms and TE = 97 ms. The 20 contiguous transverse slices with a slice thickness of 5 mm were aligned parallel to the anterior commissure and posterior commissure plane and covered all but the topmost part of the brain. The FOV was 228 $\times$ 228 mm, acquisition matrix 96 $\times$ 128, reconstructed to 128 $\times$ 128, giving a reconstructed in-plane resolution of 1.78 $\times$ 1.78 mm. For each slice, one image without diffusion weighting, and six images with

Table 1
Characteristics of the two study groups.

	Birth weight, g[a]	GA at birth, weeks[a]	Distance visual acuity, Snellen decimal mean (RE + LE)/2[a]	Socio-economic status at 14 years[b]	Age at eye exam, years[a]	Age at MRI, years[a]
VLBW (n = 30)	1234 (219) [550–1500] p 0.000	29.3 (2.8) [24–35] p 0.000	1.08 (0.29) [0.25–1.6] p 0.029	3.27 (3.5) [1–5] p 0.206	14.5 (0.37) [13.6–15.4] p 0.5	15.1 (0.62) [14.1–16.9] p 0.07
Control (n = 45)	3691 (437) [2670–4710]	39.5 (1.1) [37–42]	1.21 (0.16) [0.9–1.5.9]	3.69 (4) [2–5]	14.6 (0.49) [13.6–16.8]	15.3 (0.45) [14.2–16.4]

[a] Data given as mean (SD) [min–max values] t-test.
[b] Data given as mean (median) [min–max values] Mann Whitney test. All p values are VLBW vs. control.

diffusion gradients (b = 1000 s/mm^2) applied along six non-collinear directions were acquired. The DTI sequence was repeated six times for increased signal to noise ratio.

2.7. Calculation of diffusion tensor and scalar indices

The six DTI acquisitions acquired for each subject were first co registered to the first non-diffusion weighted volume (b_0 volume) using a mutual information cost function and a 12-parameter affine transformation. This procedure corrects for patient motion and eddy current distortions. The FLIRT program, part of the FSL program package from the Image Analysis Group, FMRIB, Oxford, UK (http://www.fmrib.ox.ac.uk/fsl), was used for the image registration. After image registration, the six acquisitions were averaged, the diffusion tensor diagonalised, and the FA maps calculated from the eigenvalues. In addition to the FA maps, the mean diffusivity (MD), the mean of the six b_0-volumes (hereafter called b_0 volume), the axial and radial diffusivity maps were calculated for each subject. Axial diffusivity, the largest eigenvalue of the diffusion tensor, measures the magnitude of water diffusion parallel to the principle diffusion direction of the voxel of interest. Radial diffusivity is the mean of the two diffusion eigenvalues perpendicular to the axial diffusion. To minimise partial volume effects from cerebrospinal fluid, voxels with a MD value greater than 2×10^{-3} mm^2/s were excluded from the diffusivity maps.

2.8. Spatial normalisation of diffusion maps

A population specific FA template was created separately for the control and VLBW groups. This avoids any bias to one of the groups due to the unequal number of subjects in the two groups. The template was created using a symmetric diffeomorphic warping algorithm implemented in the ANTS toolkit (http://picsl.upenn.edu/ANTS/). Prior to template creation, the native FA maps were resampled to 2 mm^3 isotropic resolution. The template was constructed in a similar manner as described by Kim and co-workers (2008). Default settings were used, except that the maximum number of iterations was increased to 100, and that a 4 mm search radius was used for the cross correlation similarity measure. Initial tests on the VLBW group showed that the modified settings improved the average cross correlation similarity to the derived FA template from −0.49 to −0.59. The transformation of each subject's native FA map to the template was then used to transform the b_0 images, MD maps, axial diffusion maps and radial diffusion maps to the same template space. Normalisation accuracy was assessed in two ways; by transforming the parametric maps from the regression analysis back to each subject's native space to see whether the location of the suprathreshold clusters in the parametric maps is correctly located for each subject, and by performing regression analyses on the b_0-images (see Supplementary materials and methods: Figs. S1 and S2).

2.9. Statistical analysis

The SPM8 program package (Wellcome Department of Cognitive Neurology, Institute of Neurology, London, UK, http://www.fil.ion.ucl.ac.uk/) was used for statistical analysis. The normalised diffusivity maps were smoothed with a six mm FWHM (full width at half maximum) Gaussian kernel prior to statistical analysis. An FA value of 0.15 provides a reliable threshold between grey and white matter (Jones et al., 1999), and we therefore only analysed the FA maps in the areas where all subjects included in the analysis had a FA value greater than 0.15. The linear correlation between the normalised diffusion maps (FA, MD, axial- and radial diffusion) and the different visual measurement scores were calculated in a voxel wise manner. For the analysis of the MD maps and axial and radial diffusion maps an FA > 0.15 mask was used in order to restrict the analysis to white matter. Only clusters with more than 10 contiguous voxels were reported. A significance threshold of $p < 0.001$ was used in all regression analyses.

2.10. Confirmatory ROI analysis

Once white matter areas with significant effects were identified in the exploratory VBM analysis, a confirmatory region of interest (ROI) based approach was used to further investigate the quantitative relationships between the FA values and clinical results. The ROI analysis was performed by placing a circular ROI with a radius of 2 mm (five voxels) in the centre of the anatomical area with the most significant correlation from the regression analysis. This was done in areas where it was possible to reliably place ROIs based on anatomical landmarks. The ROIs were created with MANGO version 2.3.2 (Research Imaging Center, University of Texas Health Science Centre San Antonio, USA; http://ric.uthscsa.edu/mango/). ROIs were placed on b_0-images in native space (Fig. 1). ROIs were placed such that they were at least one voxel or more from grey/white

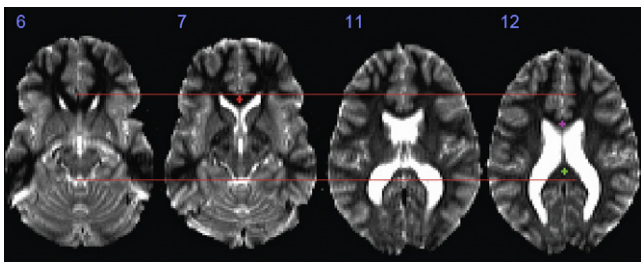

Fig. 1. Illustration of the placement of the three regions of interest (ROIs). ROIs were placed on the b_0 images in native space, and each ROI consisted of five voxels. The blue numbers refer to slice number, and the red lines indicate the positions of the poles of the genu and splenium of corpus callosum (CC). The green ROI was centred in the splenium of CC, the cyan ROI was placed approximately 1/3 from the pole of the genu of CC (midbody of CC), and the red ROI was centred in the genu of CC. (For interpretation of the references to colour in this figure legend, the reader is referred to the web version of this article.)

matter borders and not influenced by partial volume from grey matter or CSF. ROIs were then used to extract values from the various diffusivity maps in native space. From the ROI data Pearson's r was calculated for the correlation between the diffusivity data (FA, radial, axial and mean diffusion) and the visual measurements that showed a significant correlation in the exploratory VBM analysis.

3. Results

3.1. Visual acuity

Mean best corrected distance visual acuity was below 1.0 (Snellen decimals) in nine (30%) VLBW subjects, compared to four (9%) of the control subjects ($p = 0.027$, Fisher exact). The 50% in both groups performing best did not differ, as can be seen in Fig. 2, where the top performers overlap completely. However, among the worst 50% in both groups there was a significant difference ($p < 0.001$, Mann Whitney U).

3.2. FA values and visual acuity

In the VLBW group several white matter areas showed a significant positive correlation between visual acuity and FA (Fig. 3). The areas include clusters in the splenium and midbody of corpus callosum and several smaller clusters in frontal white matter. Clusters of voxels with significant correlation in all slices are shown in Fig. S3 (Supplementary material and methods). In the splenium of corpus callosum the correlation between visual acuity and FA was $r^2 = 0.36$ in the voxel with highest significance. This correlation was due to a significant negative correlation ($r^2 = 0.32$) between visual acuity and radial diffusivity. The axial diffusivity did not correlate significantly with the visual acuity ($r^2 = 0.12$, $p = 0.03$). In the mid body of corpus callosum, correlation between visual acuity and FA was $r^2 = 0.50$ in the voxel with highest significance (Fig. 3). Examining the radial and axial diffusivities at this point showed that there was a significant negative correlation with radial diffusivity ($r^2 = 0.41$) and no correlation with axial diffusivity ($r^2 = 0.09$, $p = 0.05$).

The findings in the splenium of corpus callosum were confirmed by an individually placed region of interest (ROI) analysis (Fig. 1). The ROI was centred on the hemispheric midline, and centred in the splenium of corpus callosum. FA showed a positive correlation with visual acuity ($r^2 = 0.34$, $p = 0.001$). Axial diffusivity did not correlate with visual acuity ($r^2 = 0.00$, $p = 0.969$), whereas radial diffusivity displayed a significant negative correlation ($r^2 = 0.37$, $p < 0.001$) with visual acuity. The findings in the midbody of corpus callosum were confirmed by placing a ROI approximately 1/3 from the pole of the genu of corpus callosum and in the hemispheric midline. We found that FA showed a positive correlation with visual acuity ($r^2 = 0.42$, $p < 0.001$), due to a strong negative correlation between radial diffusivity and visual acuity ($r^2 = 0.59$, $p < 0.001$). Similar to the results for the splenium, there was no correlation between visual acuity and axial diffusivity ($r^2 = 0.04$, $p = 0.711$).

For consistency we also placed an ROI in the genu of corpus callosom, where the ROI was placed in the hemispheric midline in the slice containing the most anterior point of the corpus callosum. Here we did not find that any of the diffusivity metrics FA, radial and axial diffusivity correlated with visual acuity, with all metrics showing a correlation of 0.002 or less. Graphs showing the correlation plots between visual acuity and the different diffusivity metrics in the three ROIs are included in Supplementary materials and methods (Fig. S4).

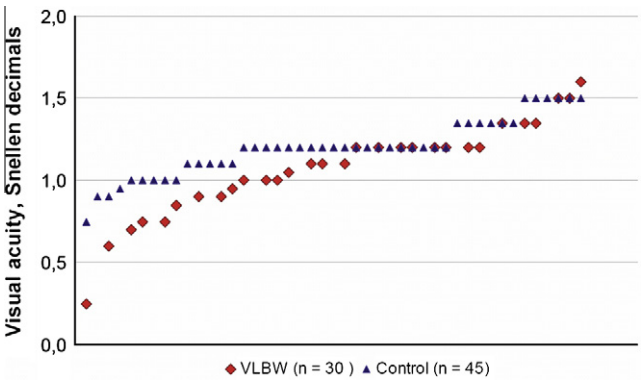

Fig. 2. Visual acuity of the participants. Best corrected distance visual acuity, mean of results of monocular testing of right and left eye. Results given as Snellen decimals where 1.0 equals 6/6 or 20/20 in Snellen decimals.

3.3. Regression analysis in the control group

In the control group, no correlations between FA and visual acuity were seen. Since the ROI analysis was done to confirm the voxel based results, no ROI analysis was done in the control group.

3.4. MD and visual acuity

No correlation was found between MD and visual acuity in either group.

3.5. Other visual variables

Near point of convergence, strabismus, stereopsis, and contrast sensitivity did not correlate significantly with FA in either group.

4. Discussion

The main finding of this study was a positive correlation between visual acuity and FA values in the corpus callosum as well as areas of frontal white matter, in preterm born VLBW adolescents. VLBW participants with low visual acuity had low FA values in the midbody and the posterior part – the splenium – of the corpus callosum. No such correlation between FA values and visual function was seen in the control group, which strengthens the assumption that the correlation in the VLBW group may be due to perinatal white matter injury related to preterm birth affecting white matter structure and connectivity.

4.1. Methodological limitations

Two methodological confounds in the present study are partial volume effects because of the relatively large slice thickness used in the DTI acquisition and inaccurate spatial normalisation in the VBM processing. We have attempted to minimise the impact of partial volume effects from CSF by applying a threshold on the raw diffusivity maps such that all voxels with a mean diffusivity greater than 2×10^{-3} mm^2/s are removed.

Voxel based morphometry is a commonly used method, well suited to study neuroanatomical correlates to neurological function and dysfunction (Ashburner & Friston, 2001; Ridgway et al., 2008). In this study a voxel-wise regression analysis comparing the FA values in the whole brain of VLBW adolescents with visual test scores was performed. A potential confounding factor in this study is inaccuracies in the spatial normalisation of the diffusion images which can lead to spurious results. We have attempted to minimise such inaccuracies by using a symmetric diffeomorphic normalisation algorithm which was reported as one of the most

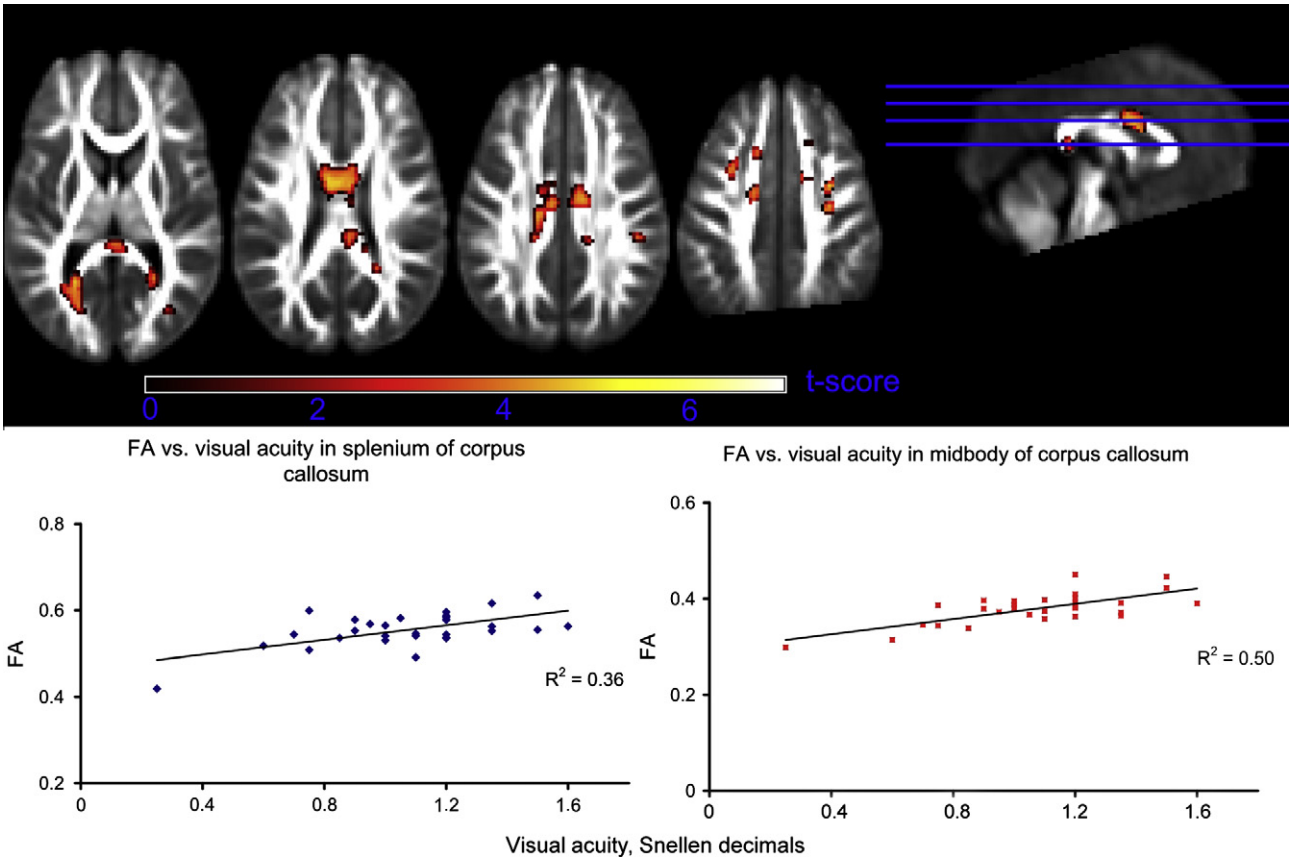

Fig. 3. White matter areas with significant correlations between fractional anisotropy (FA) values and visual acuity in the very low birth weight (VLBW) group, seen in four different transversal slices, the levels indicated on the sagittal image on the right (blue lines). Voxels with significant correlation $p < 0.001$ ($t > 3.40$) and 10 voxels cut-off are shown in yellow. The statistical map is overlaid the VLBW FA template. In the transversal slices, the left side in the image corresponds to the subject's left side (neurological convention). The colour bar represents the t score. The graphs show the linear regression plot in the most significant voxel in the splenium of corpus callosum (left) and in the midbody of corpus callosum (right). (For interpretation of the references to colour in this figure legend, the reader is referred to the web version of this article.)

accurate algorithms in a recent comparison study of 14 different algorithms (Klein et al., 2009). We further applied a threshold on the FA values (FA $\geqslant$ 0.15) that confined the analysis to white matter. We have also confirmed key findings of the VBM analysis by an independent ROI analysis. Although it was not possible to reliably place ROIs in all locations where the VBM analysis showed a correlation, the results of the ROI analysis in corpus callosum was in close agreement with the VBM results.

4.2. Relationship between preterm birth and structural white matter changes

Periventricular white matter, including the corpus callosum, is particularly prone to perinatal injury in prematurity (Volpe, 2008b). This injury seems to be mediated to a large extent by damage to pre-oligodendrocytes, a cell population particularly abundant around gestational week 23–32, and also very vulnerable to hypoxic–ischaemic and/or inflammatory processes (Back et al., 2001). Other risk factors in prematurity are vascular immaturity and low blood flow to deep cerebral white matter and in addition immature autoregulation of cerebral blood flow (Volpe, 2008a). Finally the germinal matrix in the subependymal layers of the lateral ventricles, a source of both neurons and glial cells in the developing brain is, during this period, highly vascular and prone to haemorrhage (Goldman, Geier, & Hirano, 1986; Gressens, 1992; Mo et al., 2007; Volpe, 2003). During the later half of pregnancy, the periventricular area in humans contains "crossroads areas", through which growing callosal cortico-cortical axons intersect. These crossroad areas are rich in guidance factors crucial for the spatial arrangement of axons (Judas et al., 2005). An injury in this region during the later half of pregnancy, or in the neonatal period for preterm born children, has the potential to severely disturb the midline crossing of callosal axons (Benjak et al., 2008; Deng & Elberger, 2001; Judas et al., 2005; Silver et al., 1982; Smith et al., 2006). Furthermore, preterm lesions in the subventricular zone and periventricular area may harm populations of future callosal cells directly (Gressens, 1992; Judas et al., 2005; Volpe, 1996). The vulnerability of the immature corpus callosum has also been shown in a rodent model of perinatal ischaemic–hypoxic injury: severe axonal degeneration and deterioration of fibre orientation was seen in the corpus callosum as early as 3 h after an ischaemic–hypoxic event (Skoff et al., 2001).

The thinning of the splenium often encountered in very preterm born children need not be caused by direct damage, such as described above, but could be a consequence of the general loss of periventricular white matter (Caldu et al., 2006; Nagy et al., 2003). Due to antero- and retrograde degeneration, injuries to *any* visual fibres destined to make interhemispheric connections will eventually converge in the splenium of the corpus callosum (Neil & Inder, 2006; Yoshida et al., 2004), thereby decreasing FA values in this area. However, in children born at term with unilateral perinatal periventricular white matter injury the corpus callosum is reported to be unaffected, although there may be significant changes in DTI fibre count on the lesional side, involving corticospinal tract, corticobulbar tract and superior thalamic radiation (Thomas et al., 2005). This is contrary to findings in *premature*

children, where changes in the corpus callosum are often reported as equal as or worse than those of general white matter (Caldu et al., 2006; Nagae et al., 2007; Skranes et al., 2007). This suggests that not all the damage seen in the corpus callosum of preterm born children is due to antero- and retrograde degeneration. Neuronal perinatal preterm cerebral injury appears to be more harmful for callosal fibres than injury occurring at term.

In our study, radial, but not axial diffusivity in white matter correlated to visual acuity, indicating that impaired myelination more than disturbed growth and loss of axons probably contribute to the functional impairment (Song et al., 2002, 2003, 2005).

4.3. Relationship between visual acuity and the corpus callosum

4.3.1. Splenium

It has been known for more than a century that the posterior part of the corpus callosum transfers visual information (Dejerine & Dejerine-Klumpke, 1895) and approximately 15% of all fibres originating in the occipital lobes contribute to callosal pathways (Dougherty et al., 2005). With such large amount of neural capacity devoted to the transhemispheric access of visual data, it is not surprising to find a correlation between a visual function and the microstructure of the corpus callosum. The functional importance of the splenium in transferring visual information from one hemisphere to centres (both visual and other) in the other hemisphere is well established, both through studies of patients with callosal pathology (Gazzaniga, 2000; Geschwind, 1965) and by fMRI and DTI studies in healthy volunteers (D'Arcy et al., 2006; Dougherty et al., 2005; Hofer & Frahm, 2006). Lesions of the splenium have been described to cause a range of visual problems; from pure alexia (the inability to read) (Binder & Mohr, 1992; Geschwind, 1965) to increased visual neglect in stroke patients (Bird et al., 2006) and topographical disorientation (Tamura et al., 2007).

4.3.2. Midbody and frontal white matter

Active fixation has been shown to cause increased blood flow in the frontal eye fields, the supplementary eye fields and the median cingulated gyrus in humans (Petit et al., 1995). These cortical areas are located in the vicinity of the frontal white matter areas where we find correlation between FA values and visual acuity in our study group. The regions are thought to interact to coordinate ocular fixation, eye movements and directed visual attention (Culham, Cavanagh, & Kanwisher, 2001; Petit et al., 1995), and we speculate whether the white matter areas involved are part of these networks, which are situated at the level of the midbody of the corpus callosum and are likely to use the midbody-route for interhemispheric communication. Furthermore, visual activity has been shown to lead to white matter activation in both the splenium/isthmus and the midbody of the corpus callsoum (Mazerolle et al., 2010). The observed correlation between visual acuity and FA values in the frontal white matter areas and midbody may reflect differences in ability to direct visual attention and keep steady fixation depending on the level of integrity in this area.

4.4. Visual acuity – a midline function

One distinguishing trait of visual acuity is that it is very much a midline function. This is important, since midline information is particularly favoured for callosal transfer (Berardi et al., 1989; Innocenti & Fiore, 1976; Iwamura, Taoka, & Iriki, 2001; Ptito, 2003). The highest visual acuity is achieved in the retinal fovea, defining the centre of the visual field. Here the concentration of cones is 10–20-fold higher than a few degrees peripherally (Hendrickson, 1994; Østerberg, 1935). In the optic chiasm information from both retinas, including the foveas, is split down the vertical midline, and each hemisphere receives a hemifield of visual information (Brysbaert, 2004; Leff, 2004). Integration of the two foveal visual hemifields therefore depends on some transhemispheric relay of information. If the connection, or "zipping up", of the two foveal hemifields is not optimal, the resolution could be reduced, leading to lower visual acuity. A compensatory strategy of fixating slightly to the side of the object of interest might be used; however, as the maximum resolution falls rapidly at any distance from the fovea, this will also lead to lower acuity (Anstis, 1974; Weiter et al., 1984). Thus structural integrity of the corpus callosum can be presumed to be of importance in achieving good visual acuity.

4.5. Timing of injury

It is possible that the timing of callosal injury in prematurity is important for the visual outcome. In adults experiencing callosectomy, there are to our knowledge no reports on impairments of visual acuity, but one report on "normal visual acuity" after surgery (Afraz et al., 2003). In cats there is an early critical period in the first 3 weeks after birth, where a surgical section of the corpus callosum leads to deficits in visual acuity. Lesions after this period do not affect visual acuity (Elberger, 1984). There is also evidence from rat studies that early interhemispheric communication is crucial for the functional development of visual cortex (Caleo et al., 2007). There may be a similar early sensitive period in humans, when callosal normality is particularly important for the development of good visual acuity.

4.6. Function and white matter microstructure

To our knowledge, this is the first study to show a correlation between visual acuity and FA values of the corpus callosum in preterm born children. However, it is not the first time general visual ability or other cerebral functions have been shown to correlate with callosal structure and integrity. Smaller (posterior) corpus callosum midsagittal areas, in subjects born preterm, have been associated with impaired verbal IQ (Nosarti et al., 2004), IQ and memory (Caldu et al., 2006), as well as visual motor integration (Rademaker et al., 2004). Using fMRI and conventional MRI, Santhouse and co-workers (2002) have shown different cerebral activation during visual tasks demanding callosal transfer in prematurely born young adults with callosal thinning, compared to both premature and term born control subjects without such injury. Correlations between visual ability/activity and FA values in the optic radiations have also been published: Bassi and coworkers have reported correlations between visually guided behaviour and FA values in the optic radiations at term in premature babies (Bassi et al., 2008). FA values of the optic radiations have been found to correlate significantly with fMRI measures of visual cortex activity (Toosy et al., 2004). In our study no correlation was seen between FA values and visual acuity in the control group, possibly indicating that the microstructure in a normal corpus callosum is not a limiting factor for the development of optimal visual acuity.

5. Conclusion

Our findings indicate that subnormal visual acuity in the preterm born VLBW adolescents may be related to changes in the microstructure of the midbody and splenium part of the corpus callosum seen as reduced FA values. The splenium is particularly prone to injury in prematurity. It constitutes the route for transhemispherical relay of visual information and favours foveal data. A normal splenium may contribute more to the development of

optimal visual acuity than previously acknowledged, at least in preterm born children.

Acknowledgments

The study was funded by research funds at Helse Midt-Norge, St. Olav's University Hospital, Trondheim, Norway. Part of the study population was recruited from a multicentre study sponsored by the US National Institute of Child Health and Human Development, NIH (NICHD Contract Nos. 1-HD-4-2803 and 1-HD-1-3127).

Appendix A. Supplementary material

Supplementary data associated with this article can be found, in the online version, at doi:10.1016/j.visres.2011.08.002.

References

Afraz, S. R., Montaser-Kouhsari, L., Vaziri-Pashkam, M., & Moradi, F. (2003). Interhemispheric visual interaction in a patient with posterior callosectomy. *Neuropsychologia, 41*, 597–604.

Anstis, S. M. (1974). A chart demonstrating variations in acuity with retinal position. *Vision Research, 14*, 589–592.

Ashburner, J., & Friston, K. J. (2001). Why voxel-based morphometry should be used. *Neuroimage, 14*, 1238–1243.

Back, S. A., Luo, N. L., Borenstein, N. S., Levine, J. M., Volpe, J. J., & Kinney, H. C. (2001). Late oligodendrocyte progenitors coincide with the developmental window of vulnerability for human perinatal white matter injury. *Journal of Neuroscience, 21*, 1302–1312.

Basser, P. J., Mattiello, J., & LeBihan, D. (1994). MR diffusion tensor spectroscopy and imaging. *Biophysical Journal, 66*, 259–267.

Bassi, L., Ricci, D., Volzone, A., Allsop, J. M., Srinivasan, L., Pai, A., et al. (2008). Probabilistic diffusion tractography of the optic radiations and visual function in preterm infants at term equivalent age. *Brain, 131*, 573–582.

Benjak, V., Culjat, M., Pavlovic, M., & Kostovic-Srzentic, M. (2008). Changes of the corpus callosum in children who suffered perinatal injury of the periventricular crossroads of pathways. *Collegium Antropologicum, 32*(Suppl. 1), 25–29.

Berardi, N., Bodis-Wollner, I., Fiorentini, A., Giuffre, G., & Morelli, M. (1989). Electrophysiological evidence for interhemispheric transmission of visual information in man. *The Journal of Physiology, 411*, 207–225.

Binder, J. R., & Mohr, J. P. (1992). The topography of callosal reading pathways: A case-control analysis. *Brain, 115*, 1807–1826.

Bird, C. M., Malhotra, P., Parton, A., Coulthard, E., Rushworth, M. F. S., & Husain, M. (2006). Visual neglect after right posterior cerebral artery infarction. *Journal of Neurology, Neurosurgery, and Psychiatry, 77*, 1008–1012.

Brysbaert, M. (2004). The importance of interhemispheric transfer for foveal vision: A factor that has been overlooked in theories of visual word recognition and object perception. *Brain and Language, 88*, 259–267.

Caldu, X., Narberhaus, A., Junque, C., Gimenez, M., Vendrell, P., Bargallo, N., et al. (2006). Corpus callosum size and neuropsychologic impairment in adolescents who were born preterm. *Journal of Child Neurology, 21*, 406–410.

Caleo, M., Restani, L., Gianfranseschi, L., Costatin, L., Rossi, C., Rossetto, O., et al. (2007). Transient synaptic silencing of developing striate cortex has persistent effects on visual function and plasticity. *Journal of Neuroscience, 27*, 4530–4540.

Cooke, R. W. I., Foulder-Hughes, L., Newsham, D., & Clarke, D. (2004). Ophthalmic impairment at 7 years of age in children born very preterm. *Archives of Disease in Childhood – Fetal and Neonatal Edition, 89*, F249–F253.

Counsell, S. J., Allsop, J. M., Harrison, M. C., Larkman, D. J., Kennea, N. L., Kapellou, O., et al. (2003). Diffusion-weighted imaging of the brain in preterm infants with focal and diffuse white matter abnormality. *Pediatrics, 112*, 1–7.

Crofts, B. J., King, R., & Johnson, A. (1998). The contribution of low birth weight to severe vision loss in a geographically defined population. *British Journal of Ophthalmology, 82*, 9–13.

Culham, J. C., Cavanagh, P., & Kanwisher, N. G. (2001). Attention response functions: Characterizing brain areas using fMRI activation during parametric variations of attentional load. *Neuron, 32*, 737–745.

D'Arcy, R. C., Hamilton, A., Jarmasz, M., Sullivan, S., & Stroink, G. (2006). Exploratory data analysis reveals visuovisual interhemispheric transfer in functional magnetic resonance imaging. *Magnetic Resonance in Medicine, 55*, 952–958.

Dejerine, J., & Dejerine-Klumpke, A. (1895). Corps calleux. In Rueff et cie (Ed.), *Anatomie des centres nerveux* (pp.787–803), 106, Boulevard Saint-Germain, Paris.

Deng, J., & Elberger, A. J. (2001). The role of pioneer neurons in the development of mouse visual cortex and corpus callosum. *Anatomy and Embryology, 204*, 437–453.

Dougherty, R. F., Ben-Shachar, M., Bammer, R., Brewer, A. A., & Wandell, B. A. (2005). Functional organization of human occipital-callosal fiber tracts. *The Proceedings of the National Academy of Sciences USA, 102*, 7350–7355.

Eken, P., de Vries, L., van der Graaf, Y., Meiners, L. C., & van Nieuwhuizen, O. (1995). Haemorrhagic–ischaemic lesions of the neonatal brain: Correlation between cerebral visual impairment, neurodevelopmental outcome and MRI in infancy. *Developmental Medicine and Child Neurology, 37*, 41–55.

Elberger, A. J. (1984). The existence of a separate, brief critical period for the corpus callosum to affect visual development. *Behavioural Brain Research, 11*, 223–231.

Elliott, D. B., Yang, K. C., & Whitaker, D. (1995). Visual acuity changes throughout adulthood in normal, healthy eyes: Seeing beyond 6/6. *Optometry and Vision Science, 72*, 186–191.

Fledelius, H. C. (1981). Ophthalmic changes from age of 10 to 18 years. A longitudinal study of sequels to low birth weight. II. Visual acuity. *Acta Ophthalmologica (Copenhagen), 59*, 64–70.

Frisén, L., & Frisén, M. (1981). How good is normal visual acuity? A study of letter acuity thresholds as a function of age. *Albrecht Von Graefe's Archive for Clinical and Experimental Ophthalmology, 215*, 149–157.

Gazzaniga, M. S. (2000). Cerebral specialization and interhemispheric communication: Does the corpus callosum enable the human condition? *Brain, 123*, 1293–1326.

Geschwind, N. (1965). Disconnexion syndromes in animals and man. Part II. *Brain, 88*, 585–644.

Goldman, J. E., Geier, S. S., & Hirano, M. (1986). Differentiation of astrocytes and oligodendrocytes from germinal matrix cells in primary culture. *Journal of Neuroscience, 6*, 52–60.

Gressens, P. (1992). The germinative zone produces the most cortical astrocytes after neuronal migration in the developing mammalian brain. *Biology of the Neonate, 61*, 4–24.

Hellgren, K., Hellström, A., Jacobson, L., Flodmark, O., Wadsby, M., & Martin, L. (2007). Visual and cerebral sequels of very low birth weight in adolescents. *Archives of Disease in Childhood – Fetal and Neonatal Edition, 92*, F259–F264.

Hendrickson, A. E. (1994). Primate foveal development: A microcosm of current questions in neurobiology. *Investigative Ophthalmology and Visual Science, 35*, 3129–3133.

Hofer, S., & Frahm, J. (2006). Topography of the human corpus callosum revisited – Comprehensive fiber tractography using diffusion tensor magnetic resonance imaging. *Neuroimage, 32*, 989–994.

Holmström, G., el Azazi, M., & Kugelberg, U. (1999). Ophthalmological follow up of preterm infants: A population based, prospective study of visual acuity and strabismus. *British Journal of Ophthalmology, 83*, 143–150.

Hüppi, P. S., & Dubois, J. (2006). Diffusion tensor imaging of brain development. *Seminars in Fetal and Neonatal Medicine, 11*, 489–497.

Innocenti, G. M., & Fiore, L. (1976). Morphological correlates of visual field transformation in the corpus callosum. *Neuroscience Letters, 2*, 245–252.

Iwamura, Y., Taoka, M., & Iriki, A. (2001). Bilateral activity and callosal connections in the somatosensory cortex. *Neuroscientist, 7*, 419–429.

Jacobson, L., Lundin, S., Flodmark, O., & Ellström, K. G. (1998). Periventricular leukomalacia causes visual impairment in preterm children. A study on the aetiologies of visual impairment in a population-based group of preterm children born 1989–95 in the county of Värmland, Sweden. *Acta Ophthalmologica Scandinavia, 76*, 593–598.

Jones, D. K., Simmons, A., Williams, S. C., & Horsfield, M. A. (1999). Non-invasive assessment of axonal fiber connectivity in the human brain via diffusion tensor MRI. *Magnetic Resonance in Medicine, 42*, 37–41.

Judas, M., Rados, M., Jovanov-Milosevic, N., Hrabac, P., stern-Padovan, R., & Kostovic, I. (2005). Structural, immunocytochemical, and MR imaging properties of periventricular crossroads of growing cortical pathways in preterm infants. *American Journal of Neuroradiology, 26*, 2671–2684.

Kim, J., Avants, B., Patel, S., Whyte, J., Coslett, B., Pluta, J., et al. (2008). Structural consequences of diffuse traumatic brain injury: A large deformation tensor-based morphometry study. *Neuroimage, 39*, 1014–1026.

Klein, A., Andersson, J., Ardekani, B. A., Ashburner, J., Avants, B., Chiang, M. C., et al. (2009). Evaluation of 14 nonlinear deformation algorithms applied to human brain MRI registration. *Neuroimage, 46*, 786–802.

Klingberg, T., Hedehus, M., Temple, E., Salz, T., Gabrieli, J. D. E., Moseley, M. E., et al. (2000). Microstructure of temporo-parietal white matter as a basis for reading ability: Evidence from diffusion tensor magnetic resonance imaging. *Neuron, 25*, 493–500.

Krägeloh-Mann, I., Toft, P., Lunding, J., Andresen, J., Pryds, O., & Lou, H. C. (1999). Brain lesions in preterms: Origin, consequences and compensation. *Acta Paediatrica, 88*, 897–908.

Leff, A. (2004). A historical review of the representation of the visual field in primary visual cortex with special reference to the neural mechanisms underlying macular sparing. *Brain and Language, 88*, 268–278.

Lindqvist, S., Vik, T., Indredavik, M. S., & Brubakk, A.-M. (2007). Visual acuity, contrast sensitivity, peripheral vision and refraction in low birthweight teenagers. *Acta Ophthalmologica Scandinavica, 85*, 157–164.

Lindqvist, S., Vik, T., Indredavik, M. S., Skranes, J., & Brubakk, A. M. (2008). Eye movements and binocular function in low birthweight teenagers. *Acta Ophthalmologica, 86*, 265–274.

Mazerolle, E. L., Beyea, S. D., Gawryluk, J. R., Brewer, K. D., Bowen, C. V., & D'Arcy, R. C. N. (2010). Confirming white matter fMRI activation in the corpus callosum: Co-localization with DTI tractography. *Neuroimage, 50*, 616–621.

Mo, Z., Moore, A. R., Filipovic, R., Ogawa, Y., Kazuhiro, I., Antic, S. D., et al. (2007). Human cortical neurons originate from radial glia and neuron-restricted progenitors. *Journal of Neuroscience, 27*, 4132–4145.

Nagae, L. M., Hoon, A. H., Jr., Stashinko, E., Lin, D., Zhang, W., Levey, E., et al. (2007). Diffusion tensor imaging in children with periventricular leukomalacia:

Variability of injuries to white matter tracts. *American Journal of Neuroradiology, 28*, 1213–1222.

Nagy, Z., Westerberg, H., & Klingberg, T. (2004). Maturation of white matter is associated with the development of cognitive functions during childhood. *Journal of Cognitive Neuroscience, 16*, 1227–1233.

Nagy, Z., Westerberg, H., Skare, S., Andersson, J. L., Lilja, A., Flodmark, O., et al. (2003). Preterm children have disturbances of white matter at 11 years of age as shown by diffusion tensor imaging. *Pediatric Research, 54*, 672–679.

Neil, J. J., & Inder, T. E. (2006). Detection of wallerian degeneration in a newborn by diffusion magnetic resonance imaging (MRI). *Journal of Child Neurology, 21*, 115–118.

Nosarti, C., Rushe, T. M., Woodruff, P. W. R., Stewart, A. L., Rifkin, L., & Murray, R. M. (2004). Corpus callosum size and very preterm birth: Relationship to neuropsychological outcome. *Brain, 127*, 2080–2089.

Olsen, P., Pääkö, E., Vainionpaa, L., Pyhtinen, J., & Jarvelin, M. R. (1997). Magnetic resonance imaging of periventricular leukomalacia and its clinical correlation in children. *Annals of Neurology, 41*, 754–761.

Østerberg, G. (1935). *Topography of the layer of rods and cones in the human retina* (6th ed.). Copenhagen: Levin & Munksgaard.

Petit, L., Tzourio, N., Orssaud, C., Pietrsyk, U., Berthoz, A., & Mazoyer, B. (1995). Functional neuroanatomy of the human visual fixation system. *European Journal of Neuroscience, 7*, 169–174.

Pike, M. G., Holmström, G., de Vries, L. S., Pennock, J. M., Drew, K. J., Sonksen, P. M., et al. (1994). Patterns of visual impairment associated with lesions of the preterm infant brain. *Developmental Medicine and Child Neurology, 36*, 849–862.

Ptito, M. (2003). Functions of the corpus callosum as derived from split-chiasm studies in cats. In E. Zaidel & M. Iacoboni (Eds.), *The parallel brain* (pp. 139–153). Cambridge, Massachusetts: The MTI Press.

Rademaker, K. J., Lam, J. N. G. P., Van Haastert, I. C., Uiterwaal, C. S. P. M., Lieftink, A. F., Groenendaal, F., et al. (2004). Larger corpus callosum size with better motor performance in prematurely born children. *Seminars in Perinatology, 28*, 279–287.

Reese, T. G., Heid, O., Weisskoff, R. M., & Wedeen, V. J. (2003). Reduction of eddy-current-induced distortion in diffusion MRI using a twice-refocused spin echo. *Magnetic Resonance in Medicine, 49*, 177–182.

Ridgway, G. R., Henley, S. M. D., Rohrer, J. D., Scahill, R. I., Warren, J. D., & Fox, N. C. (2008). Ten simple rules for reporting voxel-based morphometry studies. *Neuroimage, 40*, 1429–1435.

Santhouse, A. M., Ffytche, D. H., Howard, R. J., Williams, S. C. R., Stewart, A. L., Rooney, M., et al. (2002). The functional significance of perinatal corpus callosum damage: An fMRI study in young adults. *Brain, 125*, 1782–1792.

Silver, J., Lorenz, S. E., Wahlsten, D., & Coughlin, J. (1982). Axonal guidance during development of the great cerebral commissures: Descriptive and experimental studies, in vivo, on the role of preformed glial pathways. *Journal of Comparative Neurology, 210*, 10–29.

Skoff, R. P., Bessert, D. A., Barks, J. D. E., Song, D., Cerghet, M., & Silverstein, F. S. (2001). Hypoxic–ischemic injury results in acute disruption of myelin gene expression and death of oligodendroglial precursors in neonatal mice. *International Journal of Developmental Neuroscience, 19*, 197–208.

Skranes, J., Vangberg, T. R., Kulseng, S., Indredavik, M. S., Evensen, K. A. I., Martinussen, M., et al. (2007). Clinical findings and white matter abnormalities seen on diffusion tensor imaging in adolescents with very low birth weight. *Brain, 130*, 654–666.

Smith, K. M., Ohkubo, Y., Maragnoli, M. E., Rasin, M. R., Schwartz, M. L., Sestan, N., et al. (2006). Midline radial glia translocation and corpus callosum formation require FGF signaling. *Nature Neuroscience, 9*, 787–797.

Song, S. K., Sun, S. W., Ju, W. K., Lin, S. J., Cross, A. H., & Neufeld, A. H. (2003). Diffusion tensor imaging detects and differentiates axon and myelin degeneration in mouse optic nerve after retinal ischemia. *Neuroimage, 20*, 1714–1722.

Song, S. K., Sun, S. W., Ramsbottom, M. J., Chang, C., Russell, J., & Cross, A. H. (2002). Dysmyelination revealed through MRI as increased radial (but unchanged axial) diffusion of water. *Neuroimage, 17*, 1429–1436.

Song, S. K., Yoshino, J., Le, T. Q., Lin, S. J., Sun, S. W., Cross, A. H., et al. (2005). Demyelination increases radial diffusivity in corpus callosum of mouse brain. *Neuroimage, 26*, 132–140.

Tamura, I., Kitagawa, M., Otsuki, M., Kikuchi, S., Tashiro, K., & Dubois, B. (2007). Pure topographical disorientation following a right forceps major of the splenium lesion: A case study. *Neurocase, 13*, 178–184.

Thomas, B., Eyssen, M., Peeters, R., Molenaers, G., Van Hecke, P., De Cock, P., et al. (2005). Quantitative diffusion tensor imaging in cerebral palsy due to periventricular white matter injury. *Brain, 128*, 2562–2577.

Toosy, A. T., Ciccarelli, O., Parker, G. J. M., Wheeler-Kingshott, C. A. M., Miller, D. H., & Thompson, A. J. (2004). Characterizing function–structure relationships in the human visual system with functional MRI and diffusion tensor imaging. *Neuroimage, 21*, 1452–1463.

Vangberg, T. R., Skranes, J., Dale, A. M., Martinussen, M., Brubakk, A. M., & Haraldseth, O. (2006). Changes in white matter diffusion anisotropy in adolescents born prematurely. *Neuroimage, 32*, 1538–1548.

Volpe, J. J. (1996). Subplate neurons-missing link in brain injury of the premature infant? *Pediatrics, 97*, 112–113.

Volpe, J. J. (2003). Cerebral white matter injury of the premature infant – More common than you think. *Pediatrics, 112*, 176–180.

Volpe, J. J. (2008a). *Hypoxic–ischemic encephalopathy: Neuropathology and pathogenesis*. *Neurology of the newborn* (5th ed.,). Philadelphia: Saunders Elsevier.

Volpe, J. J. (2008b). *Neuronal proliferation, migration, organization, and myelination. Neurology of the newborn* (5th ed., pp. 347–399,). Philadelphia: Saunders Elsevier.

Weiter, J. J., Wing, G. L., Trempe, C. L., & Mainster, M. A. (1984). Visual acuity related to retinal distance from the fovea in macular disease. *Annals of Ophthalmology, 16*, 174–176.

Yoshida, T., Shiga, K., Yoshikawa, K., Yamada, K., & Nakagawa, M. (2004). White matter loss in the splenium of the corpus callosum in a case of posterior cortical atrophy: A diffusion tensor imaging study. *European Neurology, 52*, 77–81.